In Situ Coupled Electrochemical-Goniometry as a Tool to Reveal Conformational Changes of Charged Peptides

Amir Mohammad Ghafari, Sergio E. Domínguez, Ville Järvinen, Zahra Gounani, Amandine Schmit, Marika Sjöqvist, Cecilia Sahlgren, Outi M. H. Salo-Ahen, Carita Kvarnström, Luisa Torsi,* and Ronald Österbacka*

The opportunity to manipulate cell functions by regulating bioactive surfaces is a potentially promising approach for organic bioelectronics. Here, the tuning of the orientation of charged peptides by means of an electrical input observed via optical tensiometry is reported. A stimuli-responsive self-assembled monolayer (SAM) with specially designed charged peptides is used as a model system to switch between two separate hydrophilic states. The underwater contact angle (UCA) technique is used to measure changes in the wetting property of a dichloromethane droplet under electrical stimuli. The observed changes in the UCA of the bio-interface can be understood in terms of a change in the surface energy between the ON and OFF states. Molecular dynamics simulations in an electric field have been performed to verify the hypothesis of the orientational change of the charged peptides upon electrical stimulation. In addition, X-ray photoelectron spectroscopy (XPS) is performed to clarify the stability of the functionalized electrodes. Finally, the possibility of using such a novel switching system as a tool to characterize bioactive surfaces is discussed.

1. Introduction

Bioengineered surfaces using stimuli-responsive materials can help us understand how cells dynamically adapt to their environment and control cell functions. Various external stimuli for surface affinity modulation and manipulation of cell function have been used, which advanced the understanding of tissue engineering models and biomedical applications.[1–3] In particular, organic bioelectronics, for example, electrically responsive organic surfaces, have enabled a fast, simple, and spatiotemporal control of bio-molecular switching to facilitate the interactions of bio-functionalized electrodes and biological systems such as cells or tissue.[4,5] A bottleneck, however, is determining how to observe and track the biomolecular changes that occur on the electrodes in response to electrical stimulation.

Several groups have been utilizing switchable interfaces to dictate or regulate surface properties on demand.[5] An electroactive switchable interface is a modified electrode composed of a switchable or neutral biomolecule. When a switchable biomolecule is connected to an electrical potential source, it can activate responsive properties. A neutral biomolecule can also be switched by incorporating, for example, charged molecules or redox-active materials.[6] Hence, precise observations of the surface may elucidate molecular switching at the interface. Multiple reports mentioned the effect of electrical potentials on these switching units. For instance, surface-cell interactions are used to study switching mechanisms, which are explained by the biological output of the cells after electrical stimulation.[3,7] More direct approaches such as electrochemical surface plasmon resonance,[1,2,8,9] surface-enhanced Raman scattering,[10] in situ sum-frequency generation spectroscopy,[4]

A. M. Ghafari, V. Järvinen, Z. Gounani, L. Torsi, R. Österbacka
Physics and Center for Functional Materials
Faculty of Science and Engineering
Åbo Akademi University
Turku 20500, Finland
E-mail: ronald.osterbacka@abo.fi

S. E. Domínguez, C. Kvarnström
Turku University Centre for Materials and Surfaces (MATSURF)
Laboratory of Materials Chemistry and Chemical Analysis
University of Turku
Turku 20014, Finland

A. Schmit, M. Sjöqvist, C. Sahlgren
Cell Biology
Faculty of Science and Engineering
Åbo Akademi University
Turku 20520, Finland

O. M. H. Salo-Ahen
Pharmaceutical Sciences Laboratory, Pharmacy
Structural Bioinformatics Laboratory, Biochemistry
Faculty of Science and Engineering
Åbo Akademi University
Turku FI-20520, Finland

L. Torsi
Dipartimento di Chimica
Università degli Studi di Bari "Aldo Moro"
Bari 70125, Italy
E-mail: luisa.torsi@uniba.it

**ADVANCED
SCIENCE NEWS**
www.advancedsciencenews.com

**ADVANCED
MATERIALS
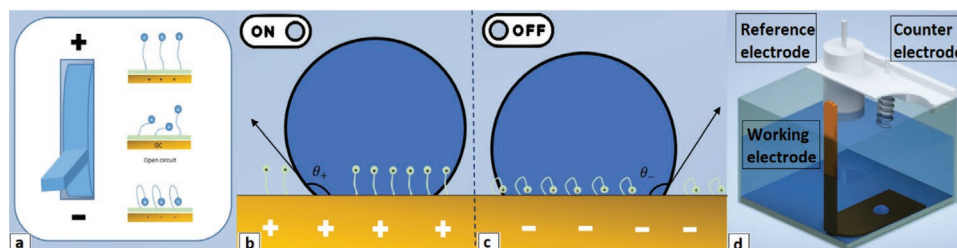INTERFACES**
www.advmatinterfaces.de

Figure 1. A schematic drawing of the in situ underwater contact angle measurement model, a) positively charged peptide modified electrode as the electro-switching surface, b) extended peptide state (ON) upon the application of positive electrical potential, and c) bent peptide state (OFF) upon the application of negative electrical potential. d) The electrochemical setup configuration.

and contact angle (CA) measurements,[11] have also been used to investigate the surface response based on switching between two (ON/OFF) states.

There is a significant potential for switchable interfaces controlling a wide range of bio-interactions and attuning interface bioactivity. Various experimental techniques have been designed and investigated[4] to demonstrate the switching mechanisms of dynamic surfaces. However, only a few reports describe the mechanistic principle behind the electrically switchable surfaces,[6] which is needed when the goal of these systems is to control their interaction with the biological systems. To approach this challenge and understand the limitation of electrically responsive surfaces, we designed an underwater contact angle (UCA) measurement (see **Figure 1**) to test and study electrically switchable surfaces in situ. This technique addresses new opportunities to the growing demand for the characterization of a responsive surface at the macro level.

While the in situ underwater contact angle measurement has been used to study the tunable wetting properties of conductive polymers during the redox reaction,[12] we hypothesize that charged peptides can alter the surface wetting properties upon a conformational change under applied bias. This paper serves as a proof-of-principle demonstration that we can control the peptide configuration by an electrical potential and monitor the changes using the underwater contact angle technique.

The rationale foresees that by applying a positive electrical potential to the peptide-functionalized electrode, the positively charged peptides are extended from the surface (ON state, Figure 1b), promoting wetting.[13] In contrast, the application of negative electrical potential attracts the positively charged peptide, which leads to bending of the peptides (OFF state, Figure 1c) and less hydrophilic surface conditions.

Combining both experimental and theoretical studies can help understand functional surfaces and facilitate the interpretation of the observed data.[14] Thus, we analyze the changes caused by the applied potential in terms of conformational changes in the peptides through underwater contact angle goniometry coupled with electrochemical measurements and molecular dynamics (MD) simulations. Our results confirm that the wetting properties are altered by the conformational change of the charged peptides on the electrode. We discuss the peptide orientation utilizing a model that introduces the possibility of in situ underwater contact angle as an easy-to-use characterization method, especially for electrically switchable bio-interfaces. Also, it presents exciting potential for the characterization of other stimuli-responsive surfaces. Such a model may apply to a wide variety of research using engineered surfaces, including cell activation platforms and biosensing.

2. Results and Discussion

2.1. In Situ Underwater Contact Angle Measurement on Bio-Functionalized Electrodes

We clarified the surface switching mechanism according to optical tensiometry, as previously demonstrated by Tsai et al.[12] A three-electrode electrochemical cell (Figure 1d) was coupled with an optical tensiometer device to measure the contact angle of the dichloromethane (DCM) droplet inside the aqueous electrolyte. Higher hydrophilicity of the extended orientation of the peptide (ON state) should lead to a higher underwater contact angle than the peptide's bent orientation (OFF state), being less hydrophilic.

First, the contact angle (CA) of a DCM droplet was precisely measured at the open circuit (OC), giving an average CA of θ = 145° ± 2° (see **Figure 2**a). Next, a positive electrical potential (+0.4 V vs. Ag/AgCl reference electrode) was applied to the electrode for 5 min while a droplet was placed next to the first one. The second droplet shows the average CA as θ = 149° ± 2°, (see Figure 2a), which is higher than for OC. Hence, a more hydrophilic surface due to the peptide being in the ON state was achieved. Finally, a third measurement was performed with a negative electrical potential (–0.2 V vs. Ag/AgCl reference electrode) was applied to the electrode. The average CA of the third droplet was θ = 138° ± 3° (Figure 2a), smaller than both the previous droplets. This can be understood because the surface is less hydrophilic when the charged peptides are bent into the OFF state.

Figure 2b, shows three droplets dispensed next to each other and their CA. We designed control experiments by preparing SAM-functionalized electrodes without the charged peptides. Similar to the conditions in Figure 2a,b, the positive and negative electrical potential was applied to the electrodes. Figure 2c,a shows that the control group is less hydrophilic than the charged peptides under OC conditions, and no change with either positive or negative potential can be observed.

We can assume that the primary driver of contact angle changes is the external electrical stimuli. The obtained results can then be used to estimate the energy difference between the two states of the switching system. Additionally, the estimation can foresee future trends in similar studies and provide quantitative data on contact angle changes.

Following Tsai et al., we can write the relationship between the contact angle and interfacial tension in a solid-liquid-liquid system (**Figure 3**) based on the Bartell-Oosterhof Equation as

$$\gamma_{DE} \cos\theta_{DE} = \gamma_{DA} \cos\theta_{DS} - \gamma_{EA} \cos\theta_{ES} \qquad (1)$$
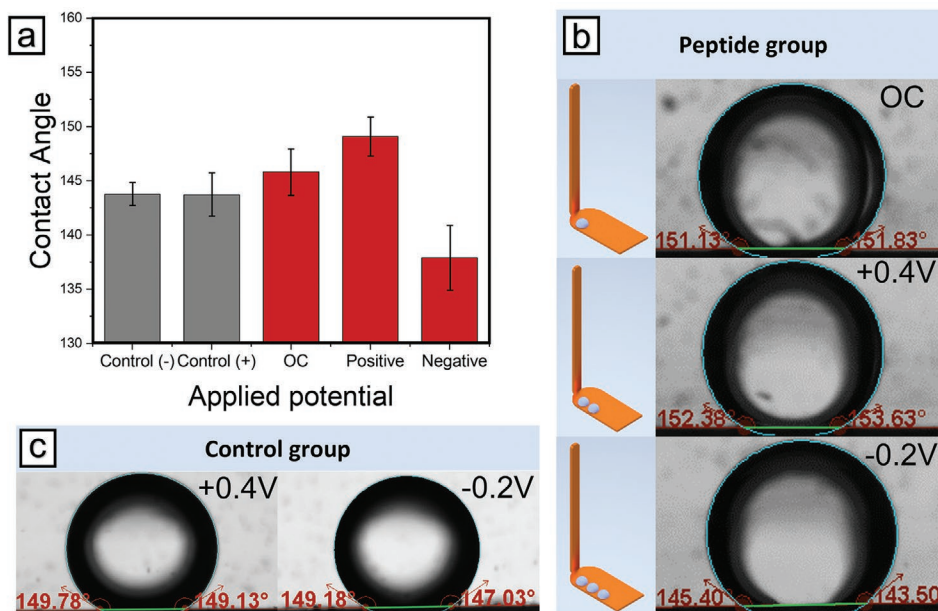
Figure 2. In situ underwater CA measurement. In a) the average CA of DCM droplets under open circuit (OC) and upon applying positive/negative electrical potential on the peptide and the control group (based on three replicates); b) the observed CA of DCM droplets (2.0 µl) on the peptide surface under OC, and upon applying +0.4 V and −0.2 V. The schematic location of the droplets is shown on the left side, and the green line (added on the original baseline of the data) represents the baseline. In c) we show the CA of DCM droplets on the control group upon applying +0.4 V and −0.2 V.

where γ_{xy} is the interfacial tension between the droplet (D), the electrolyte (E), the air (A), and the solid surface (S). Also, θ_{xy} is the contact angle of the DCM droplet within each component of the solid-liquid-liquid system. Upon applying an electrical potential at the electrode, the interfacial tension between the electrolyte ($NaNO_3$) and droplet (DCM) is constant though the surface energy changes. Therefore, the difference of surface tension between positive and negative applied potential can then be obtained from the following equation:

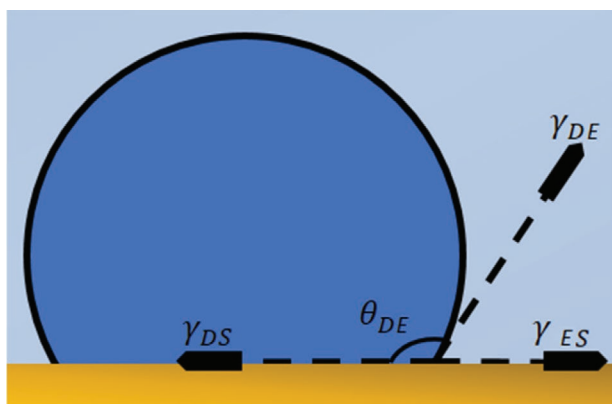$$\Delta\gamma = \gamma_{DE}(\cos\theta^-_{DE} - \cos\theta^+_{DE}) \qquad (2)$$

Figure 3. Interfacial forces on a DCM droplet in a 0.1 M $NaNO_3$ electrolyte. θ_{DE} represents the contact angle of DCM droplet, γ_{DS} the interfacial tension between the droplet and the surface. γ_{ES} is the interfacial tension between the electrolyte and the surface and γ_{DE} is the interfacial tension of the droplet and the electrolyte.

$\Delta\gamma$ is estimated based on Equations 1 and 2. The interfacial tension between DCM and the electrolyte is given as $\gamma_{DE} = 26.54 \pm 0.51$ mN m^{-1},[12] and the average contact angle of the droplets in positive (+0.4 V) and negative potential (−0.2 V) states are 149° and 138°, respectively. As a result, we obtained an estimation of the energy difference between the ON and OFF state as $\Delta\gamma = +3.57$ mN m^{-1} resulting only from the change in the applied potential. The magnitude of the change in the surface energy is in agreement with subtle changes in the ordering of films of conjugated polymers,[15] which agrees with the peptides within the SAM going into the OFF state.

Although three separate droplets were placed and measured next to each other, the performed contact angle measurements were reliable because the bio-functionalized layer was sufficiently uniform and consistent, as verified by XPS (see discussion ahead). The contact angle analyses of each electrode were consistent between different measurements and different spots on similar electrodes. In comparison, studying a single droplet under a range of applied potentials may provide incorrect results. For instance, adding and removing droplets may result in harm to the peptide-modified SAM. Given the small size of the observed alterations in CA, even a minor disturbance may cause problems.

Furthermore, the reversibility of the responsive surface in these measurements is limited. We observed that the orientational changes could only be seen when the direction of electrical potential switching goes from positive to negative and not the opposite way. It means that the contact angle is being pinned. The pinning can be caused by cations in the electrolyte drawn towards the surface each time the negative potential is applied, causing immobilization of the DCM droplet on the surface, as discussed by Tsai et al.[12]
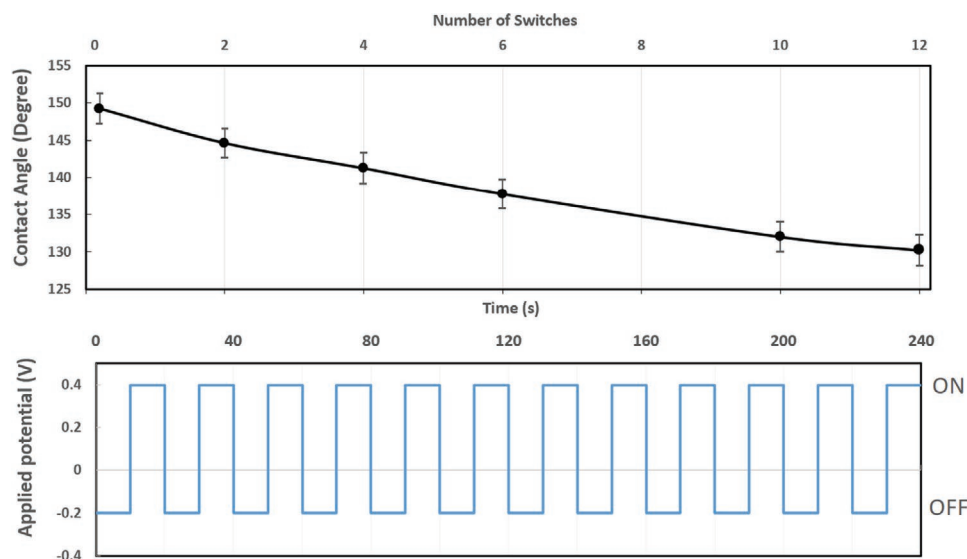
**ADVANCED
SCIENCE NEWS**

www.advancedsciencenews.com

**ADVANCED
MATERIALS
INTERFACES**

www.advmatinterfaces.de

Figure 4. The contact angle of droplets after switching the potential between positive (ON state) and negative (OFF state) for 240 seconds and in total 12 switches, the black curve indicating the contact angle versus the number of switches and, in the bottom, a schematic of the square wave potential applied to the electrodes after each measurement presented.

Another scenario could be that the peptide is drawn to the surface and (irreversibly) entangled with the underlying streptavidin/SAM. The following experiment was conducted to demonstrate how peptide gets anchored to the surface.

Here, multiple switching between positive and negative potentials was used to monitor the reversibility of the contact angle. To determine whether or not the OFF state can be switched to the ON state. The contact angle of droplets after each switching point is shown in **Figure 4**, indicating a gradual decrease. The difference in the contact angle of droplets between the last two switches is two degrees, which is within the measurement error. Hence, the repeated number of switches pins the contact angle, and it is unlikely that the ON state orientation will be reached at a later measurement stage. There is a probability that the peptide will become entangled with the surface after applying negative potentials and will result in a less oleophobic surface when switched. Also, the Marangoni effect, known to occur in similar systems due to the insoluble $NaNO_3$-ions in the electrolyte around the DCM droplet, may induce a physicochemical gradient pinning the contact angle due to uneven exposure of the film to the electrolyte cation.[12]

2.2. Molecular Modeling of the Peptide Orientational Changes

In order to verify the reactions of the charged peptides' orientational changes under the influence of an electric field, molecular dynamics (MD) simulations were employed on the same system of two peptides linked with biotin to streptavidin in a constant electric field. This is a reduced system compared to the experimental system to reduce the computational costs of the simulations. The experimental model has the SAM-functionalized gold surface in addition to the streptavidin-biotinylated peptide complexes (the SAM molecules are attached to the streptavidin molecules). Here, we assumed that the peptides

mainly interact with the large streptavidin molecule they are attached to and not so much with the underlying SAM-layer or the possibly available bare gold surface. We assumed that i) the gold electrode is evenly covered by the SAM molecules, which reduces the possibility of the peptides to adsorb onto the bare gold surface; ii) when the large streptavidin molecules evenly and tightly cover the SAM-layer, there is less space for the positively charged peptides to interact directly with the possible free carboxylic groups or the hydrophobic chain of 11-MUA and 3-MPA of the SAM-layer; and that iii) the biotin-binding sites carrying the biotinylated peptides are on the opposite side of the streptavidin protein than the SAM-attachment site because these sites would be the easiest to approach and occupy by the long peptides (this would also minimize the close contacts of the peptides with the SAM layer and the gold surface). Interestingly, in a previous MD-based computational study, it has been shown that applied electric fields (negative or positive) do not increase protein interactions with a SAM surface but rather reduce them,[16] which further supports the use of our simplified model for its intended purpose.

The simulations reveal orientational changes in the peptides upon the applied electric fields, and the changes are consistent with the expected bending and extension of the peptides. The orientational changes that the peptides undergo during the simulations with and without the applied electric fields are illustrated in **Figure 5**.

With the electric field in the upwards direction, the positively charged peptide ends are seen to move upwards, and in one out of two cases, the whole peptide is even stretched out (Figure 5c). With the electric field in the downwards direction, the peptide ends tend to bend downwards compared to the case without an electric field (Figure 5d). The graph in Figure 5a, showing the peptide's "height" (i.e., extension from the bottom of the streptavidin protein), clearly separates the three orientations of the peptide and indicates at which stages in the simulation the orientational and conformational changes happen. The
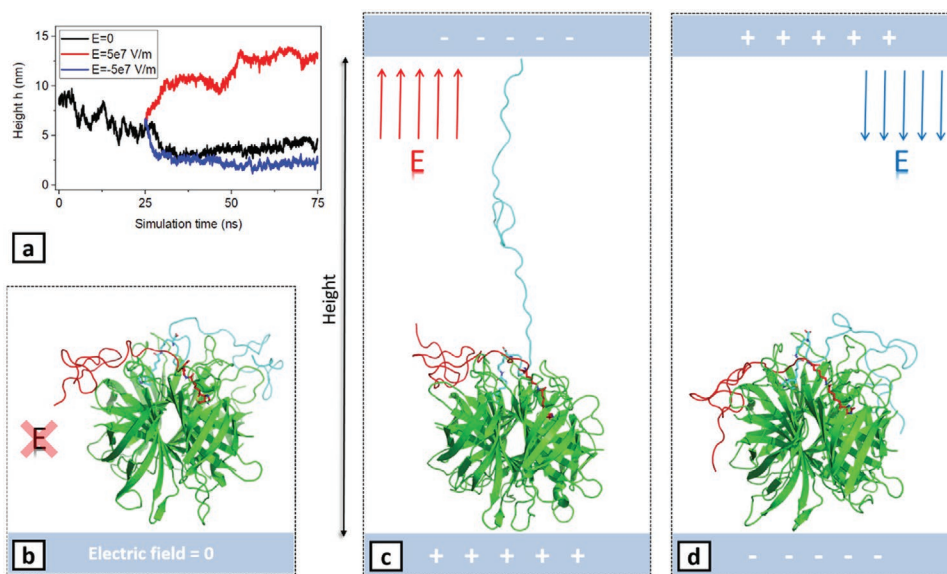
Figure 5. Orientational changes of peptides during molecular dynamics simulations with or without an electric field. The two charged peptides shown in cartoon representation (in cyan and dark red) are attached to the streptavidin protein (green, cartoon representation) via the biotin molecules (licorice presentation; atom color code: carbon–cyan/red, oxygen–red; nitrogen–blue; sulphur–yellow; hydrogen atoms are omitted for clarity). a) The "height" of the peptide (in cyan in Figure 5, b–d) (i.e., distance between the peptide's free end and the bottom of the streptavidin molecule) as a function of simulation time with and without an electric field. b) The final peptide-streptavidin complex after a 50-ns long simulation without an applied electric field and c) with an applied electric field of the strength 5×10^7 Vm^{-1} (upwards); and d) -5×10^7 Vm^{-1} (downwards). The bottom and top electrodes are depicted for clarity but are not present in the simulations. Water molecules and ions of the simulation system are not shown.

simulations further showed that in the absence of an electric field, favorable intermolecular interactions such as hydrogen bonds and the hydrophobic effect cause the peptides to fold towards the streptavidin molecule instead of letting the peptides remain somewhat extended, interacting with the water molecules. This was confirmed in the MD calculations by looking at the increasing number of hydrogen bonds forming between the peptides and the streptavidin without an electric field (see Supporting Information Figures S1 and S2). Strong favorable interactions between the peptides and the streptavidin protein may reduce the tendency of the peptides to react to electrical stimuli. In addition, this data on the number of intermolecular peptide-streptavidin hydrogen bonds showed no distinction between the cases of a downward electric field and no electric field.

Here the magnitude of the applied electric field and simulation time was determined based on studies including comparable computational details[9,17] and the expectation that the peptides might need tens of nanoseconds of simulation time to undergo any orientational changes. Simulations with different field strengths showed that with a similar but even more highly charged peptide, an electric field strength of under 10^7 Vm^{-1} would not lead to any response in the peptide over the used simulation times. Respectively, an electric field strength of over 10^8 Vm^{-1} turned out to be strong enough to dissociate the biotin molecule from the streptavidin binding site within a few nanoseconds. Thereby, a suitable magnitude of 5×10^7 Vm^{-1} was chosen for the calculations. This result demonstrates that the applied electric field should be strong enough to affect the peptides but not too strong to destroy the peptide-protein complex structure. Moreover, based on the Gouy-Chapman theory on the electrical double layer,[18] an approximation of the electric

field strength induced by the applied electrical potential in the experimental setup is calculated to be in the range 1×10^7 Vm^{-1} to 5×10^7 Vm^{-1}, indicating firstly, surface stability regarding the biotin-streptavidin dissociation and secondly, sufficiently large electric field strengths for the conformational change to occur.

As already discussed above, the accuracy of this computational modeling is limited by the absence of the SAM-layer and the electrode surface. An electrode surface in the simulations would provide a better modeling of an electrical double layer that forms in experimental setups. Further studies similar to that conducted by Xie et al.[16] may be carried out to improve the simulation's accuracy. Additionally, including a more extensive model system with ten times more peptides would increase precision, but the system size would be unreasonably large at the atomic scale, thus increasing the required computing resources significantly. Furthermore, it has been shown that a polarizable force field may provide more accurate results than a conventional force field (as used here) when the system simulated is strongly polarized in the electric field.[19] However, this modeling study depicts the nature of the peptide behavior with/without the stimuli from an electric field and is consistent with the peptide switching concept of underwater contact angle measurement suggested earlier to explain the electro switching mechanism.

2.3. XPS Analysis

XPS analysis was carried out to verify the stability of the peptide-modified SAM and to characterize the surface composition. Here, in the CA measurement method, a few factors could

**ADVANCED
SCIENCE NEWS**
www.advancedsciencenews.com

**ADVANCED
MATERIALS
INTERFACES**
www.advmatinterfaces.de

Table 1. Average chemical composition of Au, C, O, S, N of gold electrodes, control group electrodes and peptide group electrodes.

		Atomic composition (%)				
		Au	C	O	S	N
Bare gold		58.11 ± 0.4	36.8 ± 1.6	5.05 ± 1.8	–	–
Control group		33.94 ± 6.6	42.88 ± 3.9	15.49 ± 5.4	1.81 ± 0.8	5.76 ± 1.8
Peptide group	Before	23.9 ± 5.2	53.56 ± 6.0	14.16 ± 1.9	1.63 ± 0.4	6.74 ± 0.9
	After	26.3 ± 3.7	55.59 ± 3.3	10.71 ± 1.6	1.57 ± 0.3	5.72 ± 0.7

damage the surface of the electrode, such as detaching the SAM (or peptide) induced by electrical potential and unwanted reactions with DCM droplets. Therefore, XPS analysis was performed on three functionalization processes: gold electrodes, control group electrodes, and peptide group electrodes. Considering the switching unit is only on the peptide group electrodes, these electrodes were conditioned in underwater contact angle (UCA) experiments to examine the effect of electrical potential and DCM on the electrodes.

The atomic average percentages of these elements are reported in **Table 1**. Compared to the gold electrode, lower percentages of Au can be seen in the modified electrodes; on the other hand, higher percentages of carbon, oxygen, and sulfur are shown in the control and peptide groups, which indicate a successful deposition of the SAM. Additionally, the nitrogen is increased with the attachment of the bio-layers in both the control and peptide groups. All in all, these results were found to be in good agreement with previous characterization studies of the mixed SAM.[20]

Within the sensitivity of the XPS method, similar elemental compositions were obtained before and after measuring the bio-functionalized electrodes. Table 1 demonstrates the reproducibility of the functionalization and the measurement protocol. The CA measurement slightly changed the elemental compositions, although the core structure of the deposited layer stayed intact. The modified gold electrode keeps an efficient biolayer coverage before/after the measurement, verified by the reasonably constant O/Au, N/Au, S/Au ratios.

The analysis of the C1s spectrum demonstrated the stability of the peptide-modified SAM after the CA measurement. **Figure 6** presents the C1s spectrum of a peptide-modified electrode before and after the CA measurement. Three peaks were fitted on the spectrum, which demonstrated different chemical states of the surface. The red peak is the aliphatic carbons atoms of the SAM at 284.8 eV (C–H, C–C, C–COOH), the yellow and dark-blue peaks are the SAM layer (C–S, C–O), peptides, and peptide bonds (C–N, HN–C=O) at 286.4 eV and 288.2 eV. Like the before measurement condition, in Figure 6b, we demonstrated the after-measurement conditions. Likewise, peaks are located at 284.8, 286.0, and 287.9. Despite an insignificant shift in the location of the peaks, the overall conclusion is the stability of the functionalized electrodes. An equivalent stability trend was also observed in the chemical states of the surface on other elemental spectra, such as sulphur, oxygen, and nitrogen.
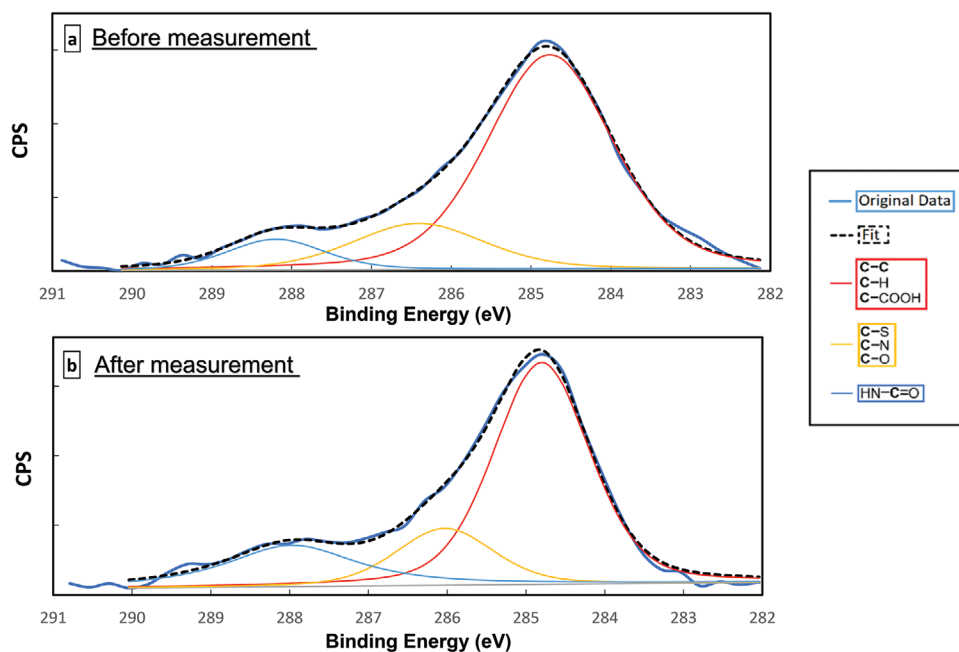

Figure 6. XPS spectra of the Carbon C1s spectrum of the peptide-modified electrode a) before and b) after CA measurements, labels are presented in the right box.

**ADVANCED
SCIENCE NEWS**
www.advancedsciencenews.com

**ADVANCED
MATERIALS
INTERFACES**
www.advmatinterfaces.de

3. Conclusions

In summary, we introduced a novel method to investigate an electro-switchable surface of charged peptides. We have shown that in situ contact angle measurement is a sensitive method to study electrically switchable peptides' configuration. As we switched the peptide between positive and negative electrical potential, the wetting properties were monitored using the contact angle of droplets on the electrodes. We show that the $\Delta \gamma$ can estimate the energy difference between the system's ON and OFF states. To the best of our knowledge, there is no available data on the extent of surface free energy changes related to such conformational changes. This might be used on various peptide-modified electro switching surfaces to assess the data trend and rationalize binding events of the surfaces with different molecules. However, further study is required to improve the sensitivity of this technique, most likely by using nano- or micropatterned surfaces.

In addition to our experimental results, XPS results confirmed the stability of the electrode during the UCA measurement, and our computational results demonstrated a similar trend for switching charged peptides upon electric field application. We demonstrate that the UCA pinning mechanism is due to the peptides forming an increased number of hydrogen bonds, as suggested by the simulations. XPS results confirmed the stability of the electrode during the UCA measurement. Our findings indicate that there is still much potential for improvement in this system, particularly concerning reversibility issues and a long-term study of the surface's stability after repeated switching. In addition, further research on different charged peptides may be carried out to deepen this concept.

Finally, based on our experimental and modeling results, this technique presents a novel way of looking at peptide configuration and opens new research opportunities for electrically switchable surfaces that can be applied to various biomodified surfaces other than peptides. We believe that this technique can be used to analyze functionalized electrodes or even bioactive materials.

4. Experimental Section

Materials: 3-MPA (≥99%),11-MUA (≥98%), EDC (≥98%), NHS (≥98%), dichloromethane (≥99.5%), NaNO3 (≥99.0%), HPLC-grade water, absolute ethanol PBS buffer tablets, 2-Propanol (≥99%), Streptavidin from *Streptomyces avidinii*, and EA hydrochloride (≥99%), were purchased from Sigma-Aldrich. Biotinylated peptide (RRRVRR RGSGSRVTCDDYYYGFGCNKFCRPRGSGSGSGSGSK-BIOTIN) was purchased from Pepmic, Suzhou, China. Positively charged amino acids are located at the distal end of the peptide. Additionally, hydrophobic, and neutral amino acids are distributed along the length of the peptide (2 negatively charged AAs, 11 positively charged AAs, 15 polar AAs, 14 hydrophobic/neutral AAs).

Functionalization of Gold Electrodes: 50 nm thick gold electrodes were prepared through thermal evaporation, followed by a cleaning process in two steps of sonication in 2-Propanol for 10 min and UV/ozone surface cleaning for 2 min. Afterward, the electrodes were quickly transferred to a glovebox and immersed into tubes containing a mixture of the thiols 3-MPA and 11-MUA (ratio of 10:1) prepared in absolute ethanol (0.01 M) to chemisorb the self-assembled monolayer.[20] Electrodes were kept inside the glovebox in the dark for 18 h at room temperature. In the Next step, functionalized electrodes were activated by the latter;

The SAM-modified gold electrodes were washed with ethanol then placed in 0.2 M EDC (N-ethyl-N'-(3-diethylaminopropyl) carbodiimide and 0.05 M NHS (N-hydroxysulfosuccinimide sodium salt) solution for 2 ho at room temperature. Then the activated electrodes were rinsed in water and immersed in a streptavidin solution (50 µg ml⁻¹ in PBS) for 2 h at room temperature for anchoring the avidin sites for avidin-biotin bonds on the functionalized electrodes. The biotin-avidin system in the previous step is identical to the one in the MD simulation. Next, ethanolamine hydrochloride solution (1 M in PBS) deactivated unreacted sites of functionalized electrodes for 1 h at room temperature. Afterward, the electrodes were rinsed in PBS and immersed in biotinylated peptide solution (50 µg ml⁻¹ in PBS) for 2 h at room temperature.

In Situ Underwater Contact Angle Measurements: In order to measure the contact angle of the DCM droplets, the following experimental setup was prepared. The bio-functionalized electrode was fixed at the bottom of a transparent cuvette as a working electrode of an electrochemical setup. The cuvette was filled with 20 ml of a 0.1 M NaNO₃ aqueous solution and placed on the stage of a Theta Lite Optical Tensiometer (C205, Attension, Biolinscientific). An Ag/AgCl reference electrode (Metrohm) and a platinum wire as the counter electrode was inserted in the cuvette and connected to an Autolab PGSTAT 101 (Metrohm) potentiostat. The electrical potential was chosen in the range +0.4 V to −0.2 V to avoid unnecessary electrochemical reactions,[2,8,21] and the contact angles of DCM droplets were measured in three steps while using the applied electrical potential of +0.2 V (ON state) or −0.4 V (OFF state) and open circuit. A droplet size between 1–5 µl is required to perform a reliable contact angle measurement.[12,22,23] We fixed the droplet size to 2 µl in volume and kept it constant throughout the measurements using an automatic droplet dispenser. First, a DCM droplet was dispensed on the electrode, and then the contact angle was measured while the circuit was kept open. A +0.2 V was applied on the electrode for 5 min in the second step, then a new droplet was dispensed next to the previous droplet, and the contact angle was recorded. Similarly, the third measurement was performed to record the contact angle of the third droplet while a −0.4 V was applied on the electrode. Four sets of measurements were performed to analyze the contact angle data, and the contact angles were recorded at 10 s with 15 FPS.

Analysis of X-Ray Photoelectron Spectroscopy: X-ray photoelectron spectroscopy analyses were carried out on a PHI Quantum 2000 XPS Microprobe spectrometer (Physical Electronics) using a monochromatic Al K(α) X-ray source, with the X-ray setting was set to 100 µm, 25 w, 15 kV. Survey scans were obtained by selected pass energy of 187.85 eV and step size of 0.8 eV for the analyzer. Furthermore, multiplex scans were acquired by selected pass energy of 58.7 eV and step size of 0.25 eV for the analyzer. These measurements were performed on three replicates, repeated in a two-cycle set and at least two spots on each sample; an electron gun was used for charge compensation during all measurements. The data was processed using the MultiPak software v. 9.9.0.

Molecular Dynamics Simulations: The MD simulations were performed with GROMACS 2019[24] simulation package using the GROMOS 54A7[25] force field parameters that were complemented with biotin parameters from the Automated Force Field Topology Builder (ATB).[26] The comparative (homology) models of the studied charged peptide was built with Modeller 9.24[27] using the peptide's primary structure (i.e., amino acid sequence) and the native Jagged1 Notch ligand structure from the Protein Data Bank[28] (PDB ID 4CC1)[29] as the template. The peptide was then covalently linked to biotin via the peptide's lysine sidechain in the C-terminus with the help of PyMOL.[30] The force field parameters for the biotinylated lysine were adapted from another study on biotinylated peptides.[31] The biotinylated peptide structures were then placed and aligned so that the biotin molecules were inside the binding pockets of a streptavidin molecule (PDB ID 1SWK).[32] The model structure consisted thus of a streptavidin molecule with two identical biotinylated peptides attached to it. Prior to running the MD simulations, energy minimization of the peptide-protein complex was run in the GROMACS environment, and the system was solvated with water molecules (SPC).[33] 12 negatively charged chloride ions were added to neutralize

**ADVANCED
SCIENCE NEWS**

www.advancedsciencenews.com

**ADVANCED
MATERIALS
INTERFACES**

www.advmatinterfaces.de

the system charge. Equilibration of the simulation system was performed for 100 ps in an NVT ensemble followed by another 100 ps in an NPT ensemble, whereafter the actual production simulations were carried out in an NPT ensemble for a total of 75 ns using the Parrinello-Rahman pressure coupling[34] and a velocity rescaling thermostat[35] at 300 K. A 2-fs timestep was used, and the cut-off radius for both the Lennard-Jones potential and the Coulomb potential in the PME method[36] was 1.2 nm. Periodic boundary conditions were defined in three dimensions as a cubic box with a side length of 13 nm. Position restraints were applied with the LINCS algorithm[37] on four nitrogen atoms on the bottom part of the streptavidin molecule to mimic the experimental setup where those nitrogen atoms could theoretically be bound with the SAM. Three production simulations were run: one completely without the applied electric field and the other two with a constant homogeneous electric field of the strength 5×10^7 Vm^{-1}. The electric field was applied in opposing directions for 50 ns in these two simulations that continued from the 25 ns structure from the simulation without the electric field. The external electric field approximated the experimentally applied electric potential. The resulting trajectories were analyzed with the GROMACS internal tools as well as with VMD.[38] Molecular visualizations and image rendering were carried out with PyMOL.

Supporting Information

Supporting Information is available from the Wiley Online Library or from the author.

Conflict of Interest

The authors declare no conflict of interest.

Data Availability Statement

The data that support the findings of this study are available from the corresponding author upon reasonable request.

[1] B. S. Gomes, E. Cantini, S. Tommasone, J. S. Gibson, X. Wang, Q. Zhu, J. Ma, J. D. McGettrick, T. M. Watson, J. A. Preece, J. C. Kirkman-Brown, S. J. Publicover, P. M. Mendes, *ACS Appl. Bio. Mater.* **2018**, *1*, 738.

[2] C. L. Yeunz, P. Iqbal, M. Allan, M. Lashkor, J. A. Preece, P. M. Mendes, *Adv. Funct. Mater.* **2010**, *20*, 2657.

[3] J. Li, Y. Lei, C. L. Sun, W. Zheng, X. Jiang, H. L. Zhang, *Adv. Mater. Interfaces* **2015**, *2*, 1.

[4] A. Pranzetti, M. Davis, C. L. Yeung, J. A. Preece, P. Koelsch, P. M. Mendes, *Adv. Mater. Interfaces* **2014**, *1*, 1400026.

[5] O. Parlak, A. P. F. Turner, *Biosens. Bioelectron.* **2016**, *76*, 251.

[6] B. S. Gomes, B. Simões, P. M. Mendes, *Nat. Rev. Chem.* **2018**, *2*, https://doi.org/10.1038/s41570-018-0120.

[7] C. C. A. Ng, A. Magenau, S. H. Ngalim, S. Ciampi, M. Chockalingham, J. B. Harper, K. Gaus, J. J. Gooding, *Angew. Chem., Int. Ed.* **2012**, *51*, 7706.

[8] A. Pranzetti, S. Mieszkin, P. Iqbal, F. J. Rawson, M. E. Callow, J. A. Callow, P. Koelsch, J. A. Preece, P. M. Mendes, *Adv. Mater.* **2013**, *25*, 2181.

[9] C. L. Yeung, X. Wang, M. Lashkor, E. Cantini, F. J. Rawson, P. Iqbal, J. A. Preece, J. Ma, P. M. Mendes, *Adv. Mater. Interfaces* **2014**, *1*, 1300085.

[10] Y. Chen, E. R. Cruz-Chu, J. C. Woodard, M. R. Gartia, K. Schulten, L. Liu, *ACS Nano* **2012**, *6*, 8847.

[11] L. Zhang, Z. Wang, J. Das, M. Labib, S. Ahmed, E. H. Sargent, S. O. Kelley, *Angew. Chem., Int. Ed.* **2019**, *58*, 14519.

[12] Y. T. Tsai, C. H. Choi, N. Gao, E. H. Yang, *Langmuir* **2011**, *27*, 4249.

[13] L. Yang, Y. Fan, Y. Q. Gao, *J. Phys. Chem. B* **2011**, *115*, 12456.

[14] E. Cantini, X. Wang, P. Koelsch, J. A. Preece, J. Ma, P. M. Mendes, *Acc. Chem. Res.* **2016**, *49*, 1223.

[15] S. E. Domínguez, A. Vuolle, M. Cangiotti, A. Fattori, T. Ääritalo, P. Damlin, M. F. Ottaviani, C. Kvarnström, *Langmuir* **2020**, *36*, 2278.

[16] Y. Xie, W. Gong, J. Jin, Z. Zhao, Z. Li, J. Zhou, *Appl. Surf. Sci.* **2020**, *506*, 144962.

[17] E. Macchia, K. Manoli, B. Holzer, C. Di Franco, M. Ghittorelli, F. Torricelli, D. Alberga, G. F. Mangiatordi, G. Palazzo, G. Scamarcio, L. Torsi, *Nat. Commun.* **2018**, *9*, 3223.

[18] H. Ohshima, *Electrical Phenomena at Interfaces and Biointerfaces: Fundamentals and Applications in Nano-, Bio-, and Environmental Sciences*, John Wiley & Sons, Hoboken **2012**.

[19] J. Zhao, X. Wang, N. Jiang, T. Yan, Z. Kan, P. M. Mendes, J. Ma, *J. Phys. Chem. C* **2015**, *119*, 22866.

[20] B. Holzer, K. Manoli, N. Ditaranto, E. Macchia, A. Tiwari, C. Di Franco, G. Scamarcio, G. Palazzo, L. Torsi, *Adv. Biosyst.* **2017**, *1*, 1700055.

[21] J. Lahann, S. Mitragotri, T.-N. Tran, H. Kaido, J. Sundaram, I. S. Choi, S. Hoffer, G. A. Somorjai, R. Langer, *Science.* **2003**, *299*, 371.

[22] J. A. Halldorsson, Y. Wu, H. R. Brown, G. M. Spinks, G. G. Wallace, *Thin Solid Films* **2011**, *519*, 6486.

[23] J. Xu, A. Palumbo, W. Xu, E.-H. Yang, *J. Phys. Chem. B* **2016**, *120*, 10381.

[24] B. Hess, C. Kutzner, D. van der Spoel, E. Lindahl, *J. Chem. Theory Comput.* **2008**, *4*, 435.

[25] W. Huang, Z. Lin, W. F. van Gunsteren, *J. Chem. Theory Comput.* **2011**, *7*, 1237.

[26] A. K. Malde, L. Zuo, M. Breeze, M. Stroet, D. Poger, P. C. Nair, C. Oostenbrink, A. E. Mark, *J. Chem. Theory Comput.* **2011**, *7*, 4026.

[27] A. Šali, *Mol. Med. Today* **1995**, *1*, 270.

[28] H. M. Berman, J. Westbrook, Z. Feng, G. Gilliland, T. N. Bhat, H. Weissig, I. N. Shindyalov, P. E. Bourne, *Nucleic Acids Res.*. **2000**, *28*, 235.

[29] C. R. Chillakuri, D. Sheppard, M. X. G. Ilagan, L. R. Holt, F. Abbott, S. Liang, R. Kopan, P. A. Handford, S. M. Lea, *Cell Rep.* **2013**, *5*, 861.

[30] Schrodinger, *The PyMOL Molecular Graphics System, Version 2.0,* LLC, **2015**.

[31] T. John, J. Bandak, N. Sarveson, C. Hackl, H. J. Risselada, A. Prager, C. Elsner, B. Abel, *Biomacromolecules* **2020**, *21*, 783.

[32] S. Freitag, I. Le Trong, A. Chilkoti, L. A. Klumb, P. S. Stayton, R. E. Stenkamp, *J. Mol. Biol.* **1998**, *279*, 211.

[33] H. J. C. Berendsen, J. P. M. Postma, W. F. van Gunsteren, J. Hermans, in *Intermolecular Forces* (Ed.: B. Pullman), Springer, Dordrecht **1981**, pp. 331–342.

[34] M. Parrinello, A. Rahman, *J. Appl. Phys.* **1981**, *52*, 7182.

[35] G. Bussi, D. Donadio, M. Parrinello, *J. Chem. Phys.* **2007**, *126*, 014101.

[36] U. Essmann, L. Perera, M. L. Berkowitz, T. Darden, H. Lee, L. G. Pedersen, *J. Chem. Phys.* **1995**, *103*, 8577.

[37] B. Hess, H. Bekker, H. J. C. Berendsen, J. G. E. M. Fraaije, *J. Comput. Chem.* **1997**, *18*, 1463.

[38] W. Humphrey, A. Dalke, K. Schulten, *J. Mol. Graphics* **1996**, *14*, 33.